

# Liquid Organic Hydrogen Carriers: Development of a Thermodynamic and Kinetic Model for the Assessment of Hydrogenation and Dehydrogenation Processes

Marco Gambini<sup>a</sup>, Federica Guarnaccia<sup>a</sup>, Maria Luisa Di Vona<sup>a</sup>, Michele Manno<sup>a,\*</sup> and Michela Vellini<sup>a</sup>

<sup>a</sup>University of Rome Tor Vergata, Via del Politecnico, 1, Rome, 00133, Italy

## ARTICLE INFO

### Keywords:

Hydrogen storage  
LOHC  
chemical kinetics  
chemical equilibrium

## ABSTRACT

Liquid organic hydrogen carriers (LOHCs) are drawing interest as a viable storage technology because of many favourable characteristics, such as high gravimetric and volumetric energy density. However, technological readiness is still limited, and very few kinetic and thermodynamic models are currently available. This paper aims to provide a complete and reliable model for the catalytic hydrogenation and dehydrogenation of a 0 H–NEC/12 H–NEC system following a general chemical thermodynamics approach that could easily extend to other LOHCs. The insurgence of already documented high-temperature phenomena has been taken into account by introducing two novel modifications to the base model, making the model reliable over a wide temperature range. First, the model identifies a maximum rate constant reached for a threshold temperature; secondly, it evaluates thermodynamic equilibrium conditions to account for a maximum H<sub>2</sub> uptake.

## 1. Introduction


Despite most countries expressing their will to achieve carbon neutrality by 2050 [1] to keep the mean global temperature increase to 1.5 °C, current trends are still lacklustre and immediate action is required to achieve this goal. To that end, the renewable energy share over the Total Primary Energy Supply (TPES) must increase by at least two thirds by 2050 [2]; in 2019, about 19.1 % of the 606 EJ [3] of the TPES were provided by either nuclear (5 % of the total) or Renewable Energy Sources (RESs).

A considerable effort is required to accommodate the overall RESs share and total energy demand increase. Each sector has to undergo profound changes, and while different strategies have been planned, not all sectors are equally easy to re-imagine.

Most RESs are intermittent and unpredictable, with a variable output that could both endanger the power system's stability and fail to meet the energy demand. Different forms of energy storage need then to be deployed: hydrogen can play a significant role since large quantities of hydrogen can be stored relatively easily for long periods, up until months in the case of seasonal storage. Stored hydrogen can supply power back to the grid to support RESs or meet energy demands in other sectors and lends itself to both centralised and decentralised solutions. While a shift toward green hydrogen production must occur, and rapid electrolyzers' up-scaling is fundamental to making green hydrogen competitive, hydrogen storage brings additional issues.

Hydrogen gas has a high Lower Heating Value (LHV) on a mass basis, but its volumetric energy density is extremely low; for instance, hydrogen and methane's LHVs are 143.0 and 55.6 MJ kg<sup>-1</sup>, respectively; however, at standard temperature and ambient pressure, the corresponding volumetric energy densities are about 0.0107 and 0.0378 MJ L<sup>-1</sup>. The two most traditional storage technologies are compressed hydrogen and liquid hydrogen: they both require a considerable amount of energy [4, 5], lead to limited energy densities and bring issues concerning materials choice, safety and vessel construction.

\*Corresponding author

 gambini@ing.uniroma2.it (M. Gambini); federica.guarnaccia@students.uniroma2.eu (F. Guarnaccia); divona@uniroma2.it (M.L. Di Vona); michele.manno@uniroma2.it (M. Manno); vellini@ing.uniroma2.it (M. Vellini)  
ORCID(s): 0000-0001-9265-5503 (M. Gambini); 0000-0002-2794-7160 (F. Guarnaccia); 0000-0002-2909-6056 (M.L. Di Vona); 0000-0001-9239-4817 (M. Manno); 0000-0002-3395-8923 (M. Vellini)

The need for a more cost-effective compact storage option has led to many alternative solutions being researched. Among the more prominent ones feature Metal Hydrides (MHs) [6, 7]. MHs usually display low volumetric and gravimetric energy densities, and their solid-state makes the design and handling of hydrogen systems more complex and less efficient than conventional solutions [8, 9].

Despite being first introduced many decades ago [10], recently, interest has sparked again around Liquid Organic Hydrogen Carriers (LOHCs) [11–13], and much effort has been devoted to assessing their performance [14–16] and optimal design configurations [17–19]. LOHCs are chemical compounds that can reversibly undergo multi-step saturation and desaturation processes of the double C-C bonds in their aromatic rings, storing and releasing hydrogen. Desaturation reactions are endothermic, thus being favoured by higher temperature levels, while saturation reactions are exothermic, so they are still kinetically favoured by high temperature, but high conversions are only reached for lower temperature levels. The volume occupied by the system increases with the gaseous moles, so hydrogen discharge is favoured by low pressure while its uptake requires higher pressure levels, as stated by the *Le Chatelier* principle. LOHC- and MH-based systems are thus very similar even if the nature of the reactions are different: LOHCs rely on actual chemical reactions, while MHs depend on physical absorption/desorption processes.

LOHCs-based systems allow for higher energy densities than MHs'. Being in a liquid phase, LOHCs allow for a more straightforward design, handling and management; moreover, it is possible to conceive an eventual integration within the current oil-derivatives infrastructure for a faster, easier and cheaper implementation.

Different compounds can serve as LOHCs with varied performances [20, 21]: cycloalkanes have relatively high hydrogen capacity, generally low toxicity and a wide liquid range; however, due to unfavourable thermodynamic properties, the operating temperature should be over 300 °C for hydrogen release. This consideration poses a limiting condition for these systems because the required reaction heat has to be provided at a moderately high temperature, thus making heat recovery less likely to occur and significantly reducing the system's overall efficiency. On the other hand, N-heterocycles sport a reduced release temperature because of a hetero-atom in the aromatic ring [22]; the required reaction enthalpy is usually lower as well, but a certain amount of hydrogen capacity is intrinsically lost. Compared to dibenzyltoluene (DBT), N-ethylcarbazole (NEC) has a similar storage capacity but a higher energy density (2.5 kWh L<sup>-1</sup> compared to 1.9 kWh L<sup>-1</sup>); its availability, stability and technical readiness are worse than DBT, but a higher gas flow, lower energy demand and dehydrogenation temperature can be granted.

As a result, DBT systems are best suited for large scale energy-transport while NEC shows considerable potential in both the energy transport and energy storage fields, but its high raw material price has to decrease to allow its diffusion.

While a model to predict the performance of DBT-based hydrogen storage systems exists [23, 24], a complete model for NEC is still missing, and the occurrence of some high-temperature phenomena during the hydrogenation phase has yet to be included in any LOHC model.

Yang et al. [25] deal with NEC dehydrogenation: kinetic equations are derived from Ref. [26]; however, the modelling procedures and results are ambiguous. Dong et al. [27] focus again on dehydrogenation, but with a different approach, analysing each reaction step instead of the overall reaction. Different catalyst performances have also been assessed by Feng and Bai [28] with a heavier focus on each reaction step, and a first-order model is provided for 1.01 bar hydrogen pressure.

Studies on hydrogenation are scarcer. Wan et al. [29] provide the currently more detailed modelling; however, the proposed model has a limited range of validity, and the final equation proposed does not match the eventual saturation of each profile for high *DoH*.

Moreover, studies currently available in the literature do not provide any analytical model on pressure dependency of NEC dehydrogenation processes. This paper thus aims to provide a complete model to describe both its hydrogen uptake and release phases, modelling the occurrence of reduced storage capability and maximum kinetic rate hinted by data provided for different compounds during hydrogenation both in liquid-state [29, 30] and gaseous-state [31–33] and ensuring the validity of the model over a wider temperature range. The model also includes the effect of pressure on both hydrogenation and dehydrogenation reaction rates.

A differential equations system can be defined to account for variable thermodynamic conditions. Such a model can be implemented to describe mass transfer over time with respect to temperature, concentration, and pressure; these results would be fundamental for assessing their techno-economical feasibility [34, 35]. While NEC is the focus of this study, the underlying research framework is entirely general and could easily be applied to describe systems based on different LOHCs once the required additional data are available.

## 2. Data

Unlike DBT, N-ethylcarbazole experimental data on pressure dependency can easily be found in the literature [29, 36]. Data are available in a pressure range of 30-70 bar and 0.25-1.00 bar for uptake and release, respectively, meaning that only relatively high or very low pressure levels are examined. On the other hand, temperature ranges overlap, which could be helpful if more advanced solutions were needed [37, 38].

### 2.1. Dehydrogenation

Dehydrogenation data are available in the literature for two different catalysts [36], with Pd/C systems yielding the best results. In this case, only three temperature levels have been studied. Even if lower temperature levels are more interesting for integration purposes, they lead to reduced kinetic performances and discharging capabilities, the reaction being endothermic. This phenomenon is most evident at relatively high pressure. It is thus apparently mandatory for any proficient NEC-based system to have a release temperature above at least 433 K, but different catalysts might lead to different results.

Data provided for the lower pressure levels have been analyzed, but whether they could be significant in any practical application is debatable. Though no information on the fitting relations was published, it is noteworthy that the dehydrogenation activation energy ( $118\text{--}127\text{ kJ mol}^{-1}$ ) is generally considerably higher than the activation energy of the uptake phase ( $\approx 27\text{ kJ mol}^{-1}$ ) [29, 39]. Graphs in Ref. [36] also indicate the actual mixture composition: it is clear that different species are favoured with respect to temperature and pressure, resulting in an additional inherent margin of error.

### 2.2. Hydrogenation

Higher pressure levels during the hydrogenation phase seem related to faster saturation, but as pressure increases, both the marginal kinetic gain and the storage capability decrease, unlike compression work. On the other hand, an increase in temperature generally leads to faster kinetics until a critical value is reached (around 433 K at 60 bar), above which a further temperature increase does not lead to any net improvement in kinetic performance, as it can be seen from the overlapping of hydrogenation profiles above 433 K profiles (see experimental data in Fig. 3a or Ref. [29]). While the presence of a maximum in the kinetic rate with respect to temperature could be unexpected, actually it features in many other hydrogenation processes for other LOHCs such as 9-ethylcarbazole (9H-NEC) [30] and also in the gaseous hydrogenation of other organic compounds such as benzene and toluene [31–33].

While no consensus has been reached on the cause of this phenomenon, different hypotheses have been proposed. The most prominent one seems to be related to reversible hydrogen desorption from the catalyst sites when a temperature around 448 K has been reached [30, 33, 40]. This hypothesis is consistent with the recurrent temperature level above which the maximum occurs for different fluids. Currently, no model has been proposed to describe this phenomenon, with all authors choosing to restrict the model's reliability to lower temperature levels.

If the temperature is even higher, the system is also affected by decreased hydrogen saturation levels (again, see the experimental data in Fig. 3a or in Ref. [29]), which means that the maximum gravimetric density is no longer 5.8 % at high temperatures. This reduction is due to thermodynamic equilibrium shifting towards the inverse reaction since the hydrogenation reaction is exothermic. A reduction in the maximum amount of stored hydrogen also occurs at the lower pressure levels, though to a lesser extent. A decreased hydrogen storage capability has been recorded for other organic substances such as 9H-NEC and toluene [30, 32] in the same temperature range but has yet to be implemented in any model.

The currently available data make it impossible to predict how both phenomena shift with temperature for different pressure levels.

The approach chosen by Wan et al. [29] to fit hydrogenation data cannot represent any dependence on the amount of hydrogenated LOHC in solution, only accounting for a mean kinetic rate. This approach does not lend itself well to describing real operating systems, in which high initial gradients significantly affect the energy balance, resulting in a different temperature level and thus different performances.

Thus, in this paper, a different approach has been followed to fit hydrogenation data, disregarding the formula proposed by Wan et al. [29], as explained in section 3.

### 3. Methods

The multi-step reaction can be studied as the equivalent single reaction starting from or leading to the fully saturated form of the LOHC species, with the effect of the liquid-gas interface and vapour pressures taken into account just for the evaluation of chemical equilibrium. These simplifying assumptions result in a simple yet reliable model, and, while a different approach could lead to slightly more accurate simulations, a model including all the reactions occurring concurrently and in sequence, together with the phases equilibrium, would be considerably more complex [23, 24] and less effective in the simulation of a whole hydrogen-based energy system.

An equation in the form of Eq. (1) has been sought to describe both kinetic rates [23, 24]. It has been proved that the rate depends on the chemical reaction only since both hydrogen transfer processes through the phase interface and the liquid medium are considerably faster [30]:

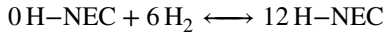
$$\frac{dX}{dt} = kf(X, n) \quad (1)$$

$$k = k_0 g(p) z(T) \quad (2)$$

with  $X$  being the amount of hydrogenated LOHC and  $n$  the reaction order.

Since for every pressure level but 60 bar, only one dataset was available, and current models do not feature any dependency in the form of  $\phi(T, p)$ , the effects of pressure and temperature were treated separately through independent functions  $g(p)$  and  $z(T)$ , according to chemical thermodynamics principles [41]. The introduction of an MH-like fictitious equilibrium pressure [42, 43] was also evaluated but yielded unsatisfactory results, demonstrating that the underlying mechanism is inherently different. If a correlation between the pressure and the system temperature exists, currently available data are not enough to define it. However, the role of pressure on the kinetic rate value is prominent, so much so that constant-temperature reactors controlled in a pressure swing fashion are regarded as forefront solutions for this technology [37, 38].

If the multi-step reaction is treated as the equivalent overall reaction:



having defined the Degree of Hydrogenation ( $DoH = n_{\text{H}_2}/n_{\text{H}_2, \text{max}}$ ) it can be directly correlated to the equivalent 12 H-NEC concentration. If  $X \equiv DoH$  for a reaction such as dehydrogenation:

$$\text{rate} = k[X]^n = -\frac{dX}{dt} \quad (3)$$

To account for the ensuing saturation effect at high  $DoH$ , the model takes into account a maximum hydrogenation level  $X_{\text{sat}}$ , evaluated with a chemical equilibrium approach, as explained later (Eqs. (12) and (13)). Thus Eq. (3) for hydrogenation and dehydrogenation turns into:

$$\left(\frac{dX}{dt}\right)_{\text{deh}} = k_{0,p,T}(X_{\text{sat}} - X)^n \quad (4)$$

$$\left(\frac{dX}{dt}\right)_{\text{hyd}} = k_{0,p,T}X^n \quad (5)$$

Even though other temperature dependencies exist for specific processes such as enzyme-regulated reactions, the most common  $z(T)$  relation comes in the form of the Arrhenius equation:

$$\ln k_{0,p,T} = \ln k_{0,p} - \frac{E_a}{RT} \quad (6)$$

If the reaction has been carried out at different temperature levels, the collected data can be used to fit Eq. (6), providing an estimation of both the apparent activation energy  $E_a$  and the frequency factor  $k_{0,p}$ .

The pressure applied to a system influences the rate constant, as well: increasing the pressure on a system at equilibrium shifts the reaction in the direction corresponding to a smaller volume, as stated in the *Le Chatelier* principle. In this work, it has been assumed that a small but essentially constant concentration of the transition state is in equilibrium with the reactants [41], having defined the transition state as the high-energy state that defines the reaction's energy barrier and is responsible for the rate constant. If the transition state occupies a smaller volume than

the reactants, a higher pressure shifts the equilibrium toward a higher concentration in the transition state, resulting in overall higher rates. This influence can be modelled through the following equation:

$$\ln k_{0,p} = -\frac{\Delta V^\ddagger}{RT}p + \ln k_0 \quad (7)$$

$$\Delta V^\ddagger = -bRT \quad (8)$$

with  $\Delta V^\ddagger$  being the activation volume.

When current models feature pressure dependencies, they either follow an exponential or a power law [24]. The latter formula was also evaluated; however, the previously explained method gave the best performance for these datasets.

The effect of temperature and pressure on the kinetic rate are thus evaluated as:

$$k = k_0 \exp(bp) \exp\left(-\frac{E_a}{RT}\right) \quad (9)$$

with exponential functions representing the effect of both pressure and temperature on the kinetic rate:  $g(p) = \exp(bp)$ ,  $z(T) = \exp(-E_a/(RT))$ .

However, with respect to the basic model here outlined, two corrections were introduced to account for the high-temperature phenomena occurring in the hydrogenation process, described in section 2. First, since a maximum kinetic rate is observed once a threshold temperature  $T_{thr}$  is reached, a simple but effective correction is proposed that sets the kinetic rate reached at temperature  $T_{thr}$  as the maximum possible rate:

$$T_{ref} = \min\{T, T_{thr}\} \quad (10)$$

$$z(T) = \exp\left(-E_a/(RT_{ref})\right) \quad (11)$$

Secondly, the decrease in hydrogen saturation level with temperature, leading to a reduced storage capability, was modelled by means of a chemical equilibrium model:

$$\Delta G_f^0 = -RT \ln(K_{eq}) \quad (12)$$

$$K_{eq} = \frac{\left([12\text{H-NEC}] \frac{p_{v,12\text{H-NEC}}}{p_0}\right)^{1/6}}{[\text{H}_2] \frac{p}{p_0} \left([0\text{H-NEC}] \frac{p_{v,0\text{H-NEC}}}{p_0}\right)^{1/6}} = \left(\frac{p_{v,12\text{H-NEC}}}{p_{v,0\text{H-NEC}}}\right)^{1/6} \frac{\zeta^{1/6} (7/6 - \zeta)}{(1 - \zeta)^{7/6} \frac{p}{p_0}} \quad (13)$$

The equilibrium constant  $K_{eq}$  can be calculated through Eq. (12) and then expressed in terms of activities, yielding Eq. (13). Data about Gibbs free energy are available in the literature [44]. The reaction takes place between the dissolved hydrogen gas and the liquid organic carrier at the catalyst sites: liquid phases have been treated as ideal (unitary activity), while LOHCs vapour pressure was evaluated through empiric laws [45]. Eq. (13) can then be solved for the reaction coordinate ( $\zeta$ ), yielding the actual maximum degree of hydrogenation  $X_{sat} \equiv DoH_{sat}$  as the ratio between the 12 H-NEC moles and the sum of 12 H-NEC and 0 H-NEC moles at equilibrium.

The proposed kinetic equations are thus:

$$\left(\frac{dX}{dt}\right)_{deh} = k_0 \exp\left(-\frac{E_a}{RT}\right) \exp(bp) X^n \quad (14)$$

$$\left(\frac{dX}{dt}\right)_{hyd} = k_0 \exp\left(-\frac{E_a}{RT_{ref}}\right) \exp(bp) [X_{sat}(T, p) - X]^n \quad (15)$$

While better results can be obtained if  $\frac{dX}{dt}$  is integrated, since datasets are provided for constant thermodynamic conditions, the results discussed in the following section were evaluated by means of numeric integration:

$$X_i \approx X_{i-1} + \left.\frac{dX}{dt}\right|_{t=t_i} \Delta t_i \quad (16)$$

because the aim of this model is to provide equations to describe real operating systems, when thermodynamic conditions are not constant.

**Table 1**

Fitting parameters of the model. Dehydrogenation parameters were obtained from 0.50-1.00 bar, while hydrogenation's cover the whole temperature and pressure given range.

Parameter	Hydrogenation	Dehydrogenation	Unit
$n$	1	2	-
$E_a$	28.07	121	$\text{kJ mol}^{-1}$
$b$	0.038	-1.220	$\text{bar}^{-1}$
$k_0$	30.33	$\approx 2.61 \times 10^{12}$	$\text{min}^{-1}$
$T_{thr}$	433	-	K

## 4. Results

Table 1 shows the numerical value of the parameters required by the model, Eqs. (14) and (15), for both dehydrogenation and hydrogenation processes, found by fitting the experimental data available in literature (see section 2). Activation energy values are consistent with those available in literature [29, 39]. The results of the fitting procedure are discussed in the next sections, separately for dehydrogenation and hydrogenation.

### 4.1. Dehydrogenation

Dehydrogenation modelling is illustrated step by step in Fig. 1. Experimental data, taken from Ref. [36], are plotted in Figs. 1a and 1b in coordinates that highlight the underlying reaction order.

Tab. 2 sums up the statistical relevance of the parameters accounting for the proposed dehydrogenation model. The normalized root square mean error (NRMSE) is defined as the ratio between the root mean square error and the mean value of each dataset. The first three rows assess the accuracy of fitting the experimental data as second-order reactions; indeed, a second-order reaction ( $n = 2$ ) suitably describes the process for all the systems held at 0.50 and 1.00 bar (Fig. 1a). However, if pressure is lowered to 0.25 bar, this correlation is lost at 473 K (Fig. 1b). Figs. 1a and 1b hint at a reaction order that is a function of both temperature and pressure. While this topic has been mostly untouched since the newly found interest in LOHCs, a varying reaction order for hydrogenation and dehydrogenation of organic compounds has already been discussed in the literature [32].

As a matter of fact, at 0.25 bar and 473 K, the best results are yielded by first-order modelling. While a second-order approximation still returns decent results in the early stages of dehydrogenation, the second-order modelling implies slower kinetics for low  $DoH$ . Consequently, any resemblance with the experimental data is lost.

Fig. 1c showcases the effect of temperature over kinetic rate for different pressure levels. At 0.50 and 1.00 bar the same angular coefficient satisfactorily fits the model, thus implying the same activation energy. Conversely, this value cannot effectively replicate the system's behaviour at 0.25 bar, where a higher activation energy value is implied if no dataset is excluded. However, if only the 433 and 453 K data at 0.25 bar are accounted for, a similar angular coefficient would be found. This is consistent with the different behaviour regarding the reaction order discussed above.

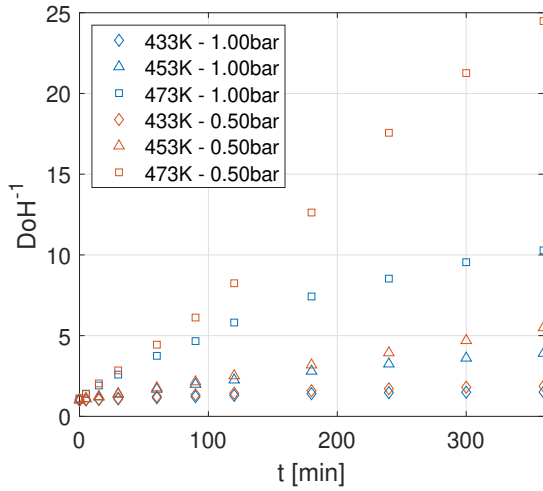
Currently, no single model features a reaction with a  $n(T, p)$  dependency, and data are too limited to suggest one.

In any case, even though low pressures yield faster discharge processes, it is unlikely that pressure levels as low as 0.25 bar or even 0.50 bar could suit the end-user requirements. Moreover, discharging trends are highly variable over time if no control strategy is in place. Since they could clash with the end-user requirements, control strategies to satisfy the end-user mass flow demand have to be set in place. Any constraints over the discharging time come from the need to match the hydrogen demand, and faster reaction kinetics are not necessarily preferable.

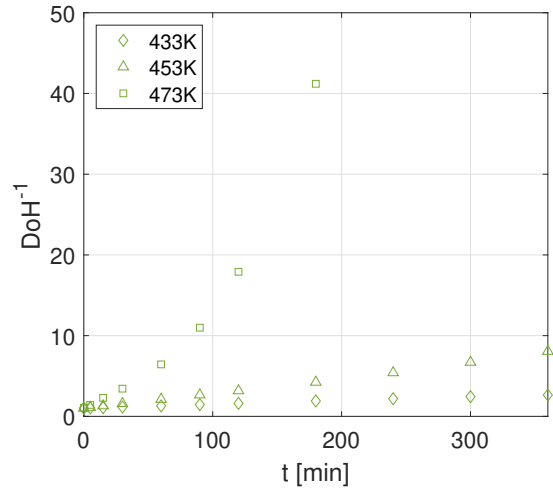
Tab. 2 shows that the fitting procedure achieves a high degree of accuracy in determining the values of activation energy  $E_a$ , pressure coefficient  $b$ , and pre-exponential factor  $k_0$ ; however, the coefficient  $b$  is calculated with only two values; thus, no NRMSE can be defined. There currently is no information about NEC's behaviour for absolute hydrogen pressure above 1.00 bar, but Fig. 1d hints at a relatively stable trend with respect to pressure, thus suggesting that the found pressure dependency could still apply for pressure levels slightly above 1.00 bar, as explained in the following.

The dehydrogenation modelling was carried out disregarding the 473 K-0.25 bar dataset. Due to the limited number of datasets available and the greatly different behaviour, its introduction would introduce considerable errors in the model (Fig. 1d).

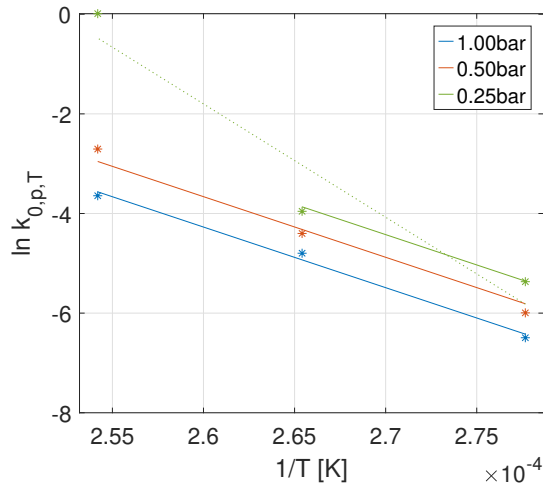




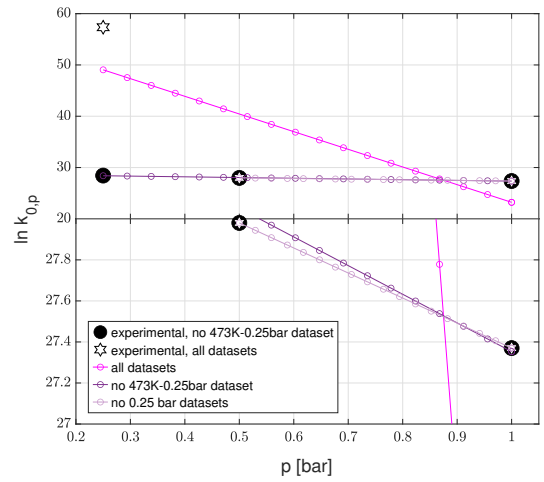
(a) Second order reaction approximation for different pressure and temperature levels.



(b) Second order reaction approximation for different temperature levels at  $p = 0.25$  bar.



(c) Temperature effect over  $k$ . The dashed line stands for the best fit equation if the 473 K-0.25 bar dataset is not discarded.



(d) Pressure effect over  $k$ . The proposed model is represented by the lilac line.

**Figure 1:** Dehydrogenation modelling results. Both Fig. 1c and Fig. 1d have  $\ln(\text{min}^{-1})$  as a unit on the y-axis .

It is evident that with only these data to work with, while the expected accuracy in the proposed range (0.25-0.50 bar and 433-453 K, 0.50-1.00 bar and 433-473 K) is still high, the error on pressure dependency's coefficient could increase quickly outside of the test conditions. However, a pressure-dependent rate equation is needed to allow for more refined control strategies, although no information is currently available for higher pressure levels.

When every dataset is included in the model, pressure dependency seems to sport a non-linear behaviour, and a sort of temperature-dependent saturation effect takes place between 0.50-1.00 bar, actually hinting at the possibility of extending the validity of the model for a limited pressure increase.

Thus, Fig. 1d showcases the effect of pressure over the rate constant; aside from the already discussed trend (magenta line), two configurations have been analysed: one of which accounts for the 433-453 K profiles at 0.25 bar (dark violet line) while the other does not feature any 0.25 bar dataset (light lilac line). The two different experimental datasets either include (white star) or exclude (black dot) the 473 K-0.25 bar data.

**Table 2**

Values of the adjusted R-squared and NRMSE for each fitting. Dehydrogenation is modelled as a second-order reaction.

		<i>p</i> / bar					
		1.00		0.50		0.25	
		$R^2_{adj}$	NRMSE	$R^2_{adj}$	NRMSE	$R^2_{adj}$	NRMSE
✕	433	0.9192	0.0451	0.9671	0.0417	0.9971	0.0197
✓	453	0.9856	0.0570	0.9997	0.0109	0.9978	0.0334
⌢	473	0.9615	0.1268	0.9969	0.0508	0.6724	1.1009
$E_a, k_{0,p}$		0.9975	0.0210	0.9908	0.0220	0.9165	0.3672
$b, k_0$						1	-

While accounting for the dataset mentioned above leads to a drastically different set of coefficients, including the two low-temperature configurations at 0.25 bar leads to only a limited variation.

In the end, the model here proposed only includes the 0.50 and 1.00 bar data. These data were chosen because, despite relying on a smaller data pool, they provide a better performance both in the 0.50-1.00 bar range (as expected) and ultimately for  $p = 0.25$  bar as well.

Conversely, if the two lowest temperature levels at 0.25 bar are considered, the same activation energy  $E_a$  used for the higher pressure systems is still valid (Fig. 1c), but the newly found  $\ln k_0$  and  $b$  display small variations from the original values. If only the actual outlier at 0.25 bar is excluded from the model, the absolute value of  $b$  increases by 14.51% while  $k_0$  increases by 17.30% despite the actual fitting parameter obtained<sup>1</sup> only increasing by 0.55%.

It must also be reiterated that the limited amount of sampling points leads to relatively high  $R^2$  even for the 0.25 bar and 473 K profile, but looking at the graphs (Fig. 1b) it is evident that significant errors are introduced. NRMSE values, therefore, give a better representation of the fit accuracy.

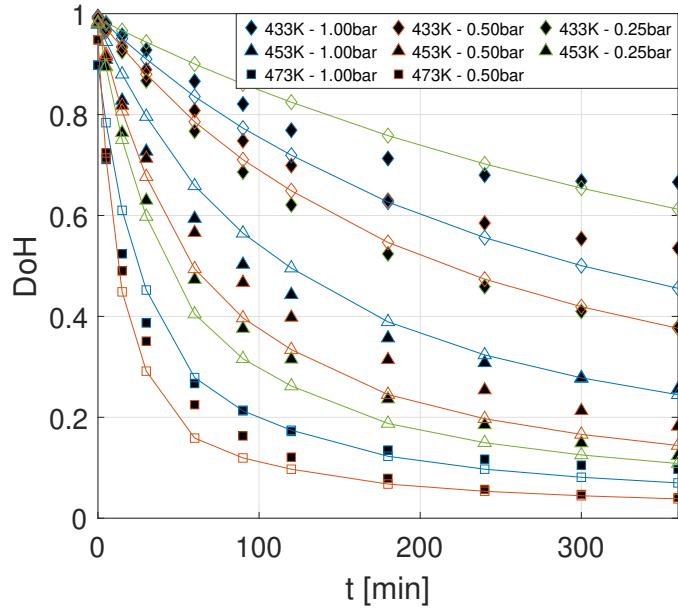
Fig. 2a shows the time evolution of the degree of hydrogenation, comparing numerically obtained results with experimental data: an overall good agreement is reached, in line with the accuracy of the fitting procedure discussed above. Fig. 2b sums up the errors introduced by the model for the proposed parameter set and the one obtained excluding the high-temperature, low-pressure profile. The statistical parameter on the y-axis is evaluated as the sum of all relative errors between numerical and experimental data.

While the two models yield similar performances at 1.00 bar, the introduced error at 0.50 bar grows as temperature increases. Lowering the pressure, at 433 K the second model (violet marker) leads to extremely low errors, but at 453 K its performances plummet. On the other hand, the first model (lilac marker) has only slightly worse performances at 433 K but fares considerably better at 453 K.

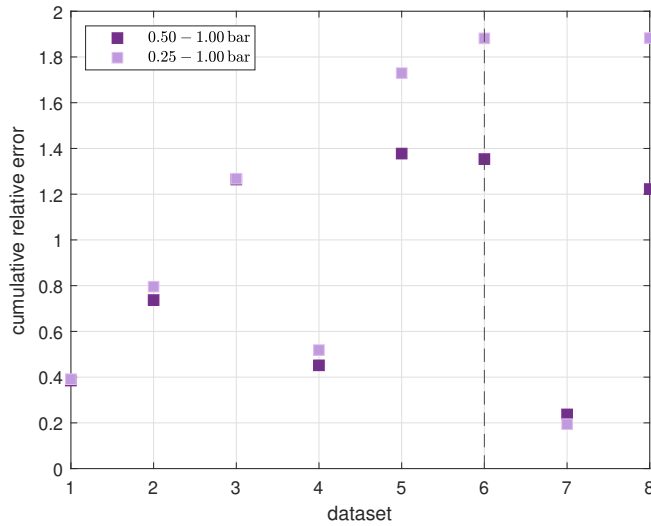
All things considered, the chosen model yields more than satisfactory performances. However, a denser and wider data pool is required to better characterize the hydrogen-release process behaviour. Including or excluding data at 0.25 bar leads to similar coefficients, proving the model's reliability inside and slightly outside of the base test conditions. However, the resulting magnitude of  $k_0$  is so high that it single-handedly makes the dehydrogenation phase more vulnerable to errors than hydrogenation (see Section 4.2).

<sup>1</sup>The procedure returns  $\ln k_0$ .





(a) Dehydrogenation modelling for 0.25-1.00 bar systems using the lilac model (Fig. 1d). Lines with empty markers: model results; filled markers: experimental data.



(b) Measure of the introduced error. Datasets identified as 1-3 refer to systems held at increasingly high temperature and 1.00 bar. Datasets identified as 4-6 refer to systems held at increasingly high temperature and 0.50 bar. The last two datasets are the 433 and 453 K systems at 0.25 bar.

**Figure 2:** Dehydrogenation modelling results.

**Table 3**

Values of the adjusted R-squared and NRMSE for each fitting. Hydrogenation is modelled as a first-order reaction.

$p = 60 \text{ bar}$	$T / \text{K}$	$R^2_{adj}$	NRMSE
	368	0.9887	0.1060
	378	0.9504	0.1804
	393	0.9919	0.0643
	403	0.9826	0.0852
	433	0.9833	0.0504
	453	0.8912	0.0909
	468	0.9571	0.1165
	483	0.7846	0.2120
	493	0.7695	0.1976
$T = 433 \text{ K}$	$p / \text{bar}$	$R^2_{adj}$	NRMSE
	30	0.9318	0.1949
	40	0.9858	0.0970
	50	0.9895	0.0602
	60	0.9833	0.0504
	70	0.9930	0.0315
$E_a/k_{0,p}$		0.9345	0.0700
$b, k_0$		0.9151	0.0663

## 4.2. Hydrogenation

Tab. 3 showcases the statistical parameters that define the modelling process for the hydrogenation phase. Hydrogenation profiles were included in the modelling procedure only up to the onset of saturation; however, the profiles represented in Fig. 3a show the full experimental dataset.

Fig. 3 provides information about each modelling step. Namely Fig. 3a and Fig. 3b highlight the validity of the first-order approximation, which results in a straight line with the chosen coordinates: experimental data fit well (Tab. 3) until saturation conditions are reached. When saturation is reached, the angular coefficients change, and each profile turns into a horizontal line. Being a pseudo-first-order reaction, it is likely that the excess reagent does not influence the kinetic, so much so that Eq. (4) effectively correlates the rate to the unsaturated LOHC concentration.

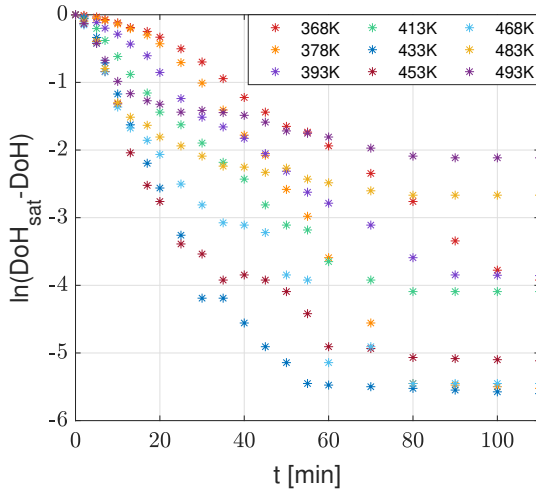
Fig. 3c and Fig. 3d highlight the validity of Eqs. (6) and (7) respectively. The positive angular coefficient in Fig. 3d was expected due to the beneficial effect of pressure over the kinetic rate; the trend portrayed in Fig. 3c can instead be explained by the limited influence of temperature on rate for  $T \geq 433 - 453 \text{ K}$ . Experimental datasets clearly point to a threshold level above which the beneficial effect of temperature increase on kinetic rate is counterbalanced by additional mechanisms unlocked at high temperature, as discussed in section 2.

Looking at the slope of the higher temperature profiles, it is evident that for temperature above  $\approx 433 - 453 \text{ K}$  gradients do not get increasingly steeper as the temperature gets higher, as expected if Eq. (6) were to hold over the whole temperature range. Indeed, the Arrhenius dependency imposed on the experimental data would imply that as temperature increases, the activation energy would eventually be null and then negative since the angular coefficient of the fitting in Fig. 3c is proportional to activation energy:  $m = -E_a/R$ .

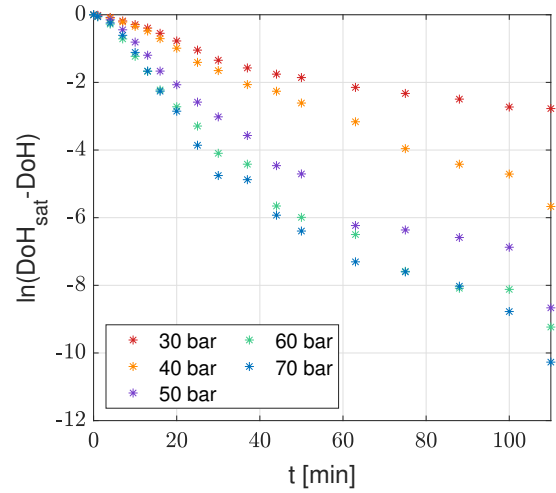
The maximum value of  $DoH$  calculated with Eqs. (12) and (13) as a function of pressure and temperature, compared to experimental data available in the literature, is represented in Fig. 4.

Some error is introduced for lower temperature values but with little to no practical consequence on the overall effectiveness of the model. On the other hand, the correction enables the model to assess the system performance with good accuracy at higher temperatures and lower pressures.

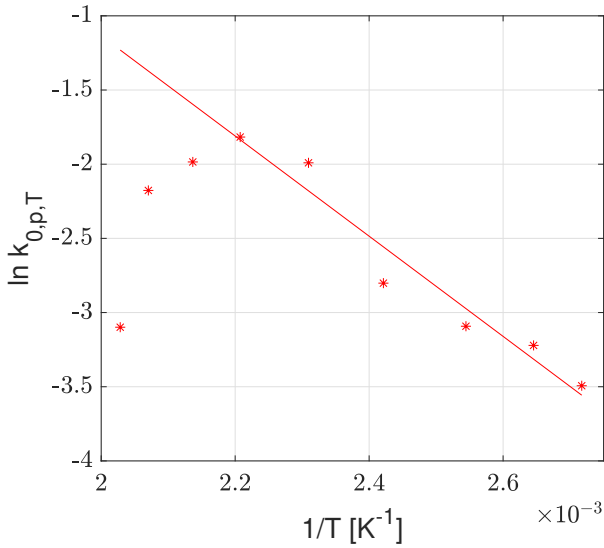
As long as  $T < 468 \text{ K}$  there is no evidence of any storage capacity drop, so if Eq. (13) is taken into account for any temperature level, slight errors may be introduced in the lower temperature range. This discrepancy is not only slight, leading to a minimal deviation as seen in Fig. 5a, but does not influence a real operating system because the storage system would not be filled up to saturation conditions but up to a lower degree of hydrogenation, usually limited to  $DoH_f = 0.9 - 0.95$  [23, 24], to avoid going through the slow saturation phase. Thus, no deviation is introduced for a  $DoH$  range of practical interest.



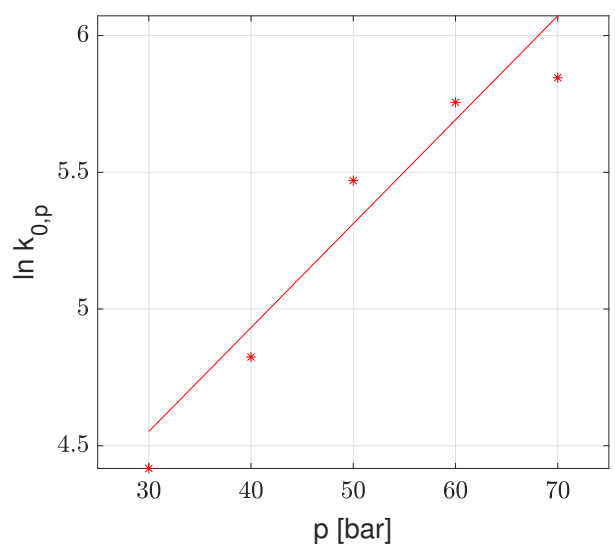
(a) First order reaction approximation for different temperature levels and  $p = 60$  bar.



(b) First order reaction approximation for different pressure levels and  $T = 433$  K.



(c) Temperature effect over  $k$ .



(d) Pressure effect over  $k$ .

**Figure 3:** Hydrogenation modelling results. Both Fig. 3d and Fig. 3c y-axis have  $\ln(\text{min}^{-1})$  as a unit.

Further analyses on the equilibrium conversion will be done in future works, accounting for the multi-step reaction. However, given the limited amount of available data to support any theory in conjunction with a satisfactory adherence to data, the proposed model was deemed more than adequate.

A different approach was chosen in other works [46], where no pressure correction was given, and the actual reaction order was not taken into consideration [47]. Recently, the issue was addressed for DBT [48]; however, in that case, equilibrium conditions were simply evaluated through a fitting procedure and not through a chemical thermodynamic model.

Both high-temperature corrections are thus essential to accurately reproduce the experimental data over a wide range of operating conditions, even though they are not strictly necessary for low-temperature and high-pressure systems.

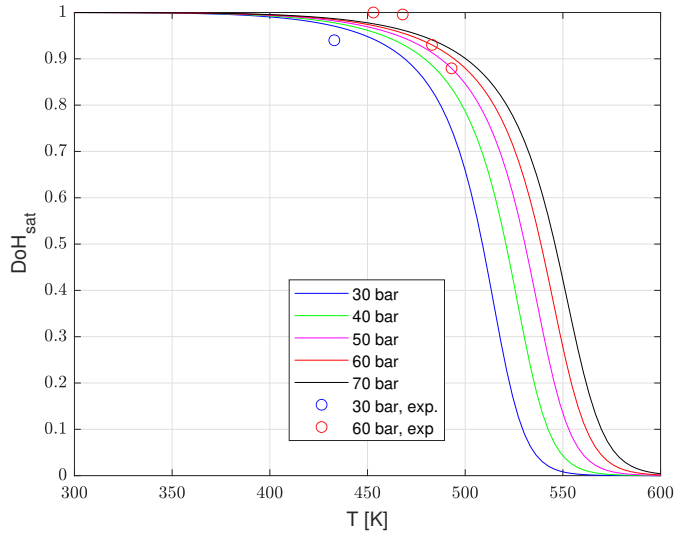
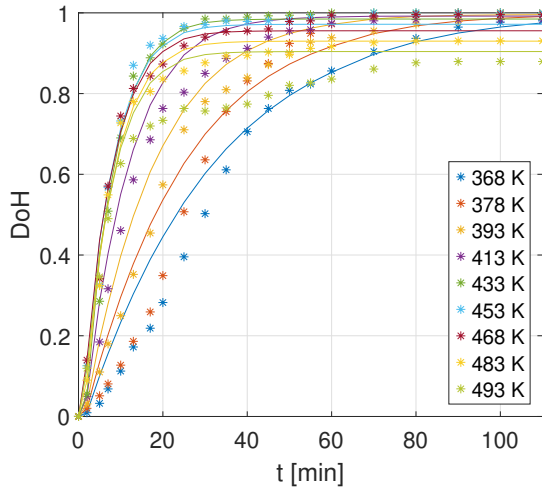
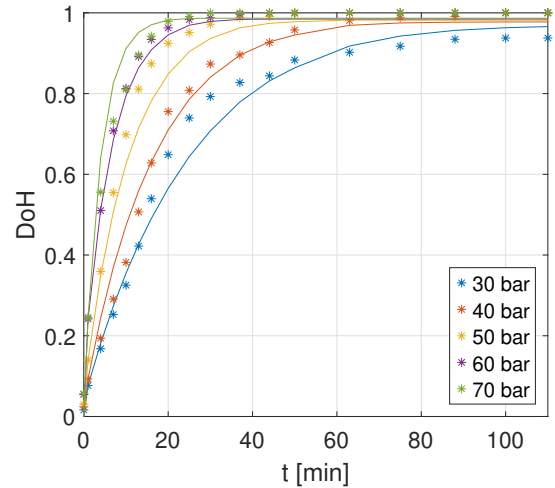


**Figure 4:**  $DoH_{sat}$  profiles resulting from Eq. (13).



(a) Experimental and modelled data for  $p = 60$  bar.



(b) Experimental and modelled data for  $T = 433$  K.

**Figure 5:** Hydrogenation modelling results; lines: model results; markers: experimental data.

Looking at Fig. 5a it is clear that after the introduction of both corrections, represented by Eqs. (10)–(13), the model introduces the greatest error for low to middle  $DoH$  in the 368 and 378 K profiles. Not only is this error definitely lower than the one caused by the base model at higher temperatures, but these temperature levels would lengthen the charging times considerably, making them much less relevant than the temperature profiles  $T \geq 398$  K. Moreover, the hydrogenation reaction is exothermic, so in an actual system, the temperature would initially increase, making the inaccuracy of the model in the first stages of hydrogenation at a constant low temperature irrelevant: it is indeed reasonable to assume that when the system temperature decreases, the achieved  $DoH$  would be sufficiently high to avoid the larger errors.

The system performance significantly improves as temperature increases until it reaches about 453 K and errors would quickly increase again if both corrections were not in place. This is due to the resurgence of the two previously explained high-temperature phenomena. Lacking both, Wan et al. [29] limit the validity of their model to low temperate

levels. It is also worth mentioning that the overall charging time, which the model effectively predicts, might arguably be more important than the hydrogenation profile.

Pressure dependency yields overall good results, with the worst performance for the system held at 70 bar. Fig. 5b suggests that the model's accuracy may drop quickly at higher pressures. The provided data suggest that a pressure increase leads to some kinetic gain until a specific threshold value is reached, but this limit is not particularly concerning because systems can be held at constant pressure, and there is neither a kinetic nor energetic gain in raising pressure above 60 bar. In order for LOHC-based systems to be effective, hydrogen should not be compressed beforehand; thus, pressure levels should be around 10-50 bar, which is a reasonable operating range for water electrolyzers [23].

For 30 bar systems, the maximum amount of hydrogen that can be stored drops to about 94%, which means that chemical equilibrium should necessarily be factored in to provide accurate results. An increasingly greater influence is expected at even lower pressure levels, as predicted by the model.

## 5. Conclusions

For the dehydrogenation process, overall fairly accurate models were obtained, accounting for both temperature and pressure dependencies. However, their validity is tied to a relatively tight range of thermodynamic conditions due to the relative lack of data. Due to inconsistent behaviour in terms of the reaction order under different thermodynamic conditions, a denser and greater data-pool would benefit the model's reliability. Ultimately, the proposed model was calibrated with data based on just the 0.50 and 1.00 bar pressure profiles. It does provide with more than decent performance even extrapolating data at 0.25 bar, proving that the stability of the underlying chemical-kinetic model.

Future works could focus on the development of a functional relationship between the reaction order  $n$  and the system's thermodynamic conditions, and on the evaluation of the system's behaviour during dehydrogenation at relatively high pressure.

In the case of hydrogenation, the model yielded excellent results and allowed for an exhaustive characterisation. Accuracy is relatively low at low temperatures (368 and 378 K) and high pressures (70 bar); however, errors are still very limited and those conditions are not optimal for practical applications. Moreover, at these temperatures, the model loses accuracy only for medium-low hydrogen content, that is, in the first stage of the hydrogenation process, when the LOHC heats up significantly, well above those temperature levels. On the other hand, operating the system at 70 bar would only require higher energy costs and stresses on materials without any substantial benefit.

If the system temperature is above 433-453 K, a simple kinetic model cannot describe the hydrogenation process accurately. Two novel correction factors were introduced to extend the validity of the model. The proposed model takes into account both the lack of further speeding up in the kinetic rate and the reduced storage capacity with simple modifications to the base equation. Alternative approaches were not found in the literature, and while more complex solutions could be sought, the model already provides excellent adherence to experimental data.

This article is intended to be the foundation for future works, which will focus on the whole thermodynamic system consisting of a reactor containing the LOHC and providing both a hydrogen inlet or outlet and an external fluid to reduce the temperature peak (hydrogenation) or drop (dehydrogenation).

## CRedit authorship contribution statement

**Marco Gambini:** Conceptualization, Methodology, Supervision. **Federica Guarnaccia:** Methodology, Software, Validation, Writing - Original Draft, Writing - Review & Editing, Visualization. **Maria Luisa Di Vona:** Methodology, Supervision. **Michele Manno:** Methodology, Validation, Writing - Original Draft, Writing - Review & Editing, Visualization. **Michela Vellini:** Methodology, Validation, Writing - Review & Editing, Visualization.

## References

- [1] International Energy Agency. Net Zero by 2050 - A Roadmap for the Global Energy Sector, 2021. URL <https://www.iea.org/reports/net-zero-by-2050>. Last retrieved on 14/02/2022.
- [2] International Renewable Energy Agency. Global energy transformation: A roadmap to 2050, 2019. URL <https://www.irena.org/publications/2019/Apr/Global-energy-transformation-A-roadmap-to-2050-2019Edition>. Last retrieved on 14/02/2022.
- [3] International Energy Agency. Total primary energy supply by fuel, 1971 and 2017. URL <https://www.iea.org/data-and-statistics/charts/total-primary-energy-supply-by-fuel-1971-and-2017>. Last retrieved on 18/01/2022.
- [4] U.S. Department of Energy. Energy requirements for hydrogen gas compression and liquefaction as related to vehicle storage needs, 2009. URL [https://www.hydrogen.energy.gov/pdfs/9013\\_energy\\_requirements\\_for\\_hydrogen\\_gas\\_compression.pdf](https://www.hydrogen.energy.gov/pdfs/9013_energy_requirements_for_hydrogen_gas_compression.pdf).

- [5] Andreas Züttel, Arndt Remhof, Andreas Borgschulte, and Oliver Friedrichs. Hydrogen: the future energy carrier. *Philosophical Transactions of the Royal Society A: Mathematical, Physical and Engineering Sciences*, 368(1923):3329–3342, 2010. doi: 10.1098/rsta.2010.0113.
- [6] M Gambini, M Manno, and M Vellini. Numerical analysis and performance assessment of metal hydride-based hydrogen storage systems. *International Journal of Hydrogen Energy*, 33(21):6178–6187, 2008. doi: 10.1016/j.ijhydene.2008.08.006.
- [7] Marco Gambini, Tommaso Stilo, and Michela Vellini. Hydrogen storage systems for fuel cells: Comparison between high and low-temperature metal hydrides. *International Journal of Hydrogen Energy*, 44(29):15118–15134, 2019. doi: 10.1016/j.ijhydene.2019.04.083.
- [8] Marco Gambini, Tommaso Stilo, and Michela Vellini. Selection of metal hydrides for a thermal energy storage device to support low-temperature concentrating solar power plants. *International Journal of Hydrogen Energy*, 45(53):28404–28425, 2020. doi: 10.1016/j.ijhydene.2020.07.211.
- [9] Marco Gambini, Tommaso Stilo, and Michela Vellini. High temperature metal hydrides for energy systems Part B: Comparison between high and low temperature metal hydride reservoirs. *International Journal of Hydrogen Energy*, 42(25):16203–16213, 2017. doi: 10.1016/j.ijhydene.2017.03.227.
- [10] M Taube, D Rippin, D Cresswell, and W Knecht. A system of hydrogen-powered vehicles with liquid organic hydrides. *International Journal of Hydrogen Energy*, 8(3):213–225, 1983. doi: 10.1016/0360-3199(83)90067-8.
- [11] Daniel Teichmann, Wolfgang Arlt, and Peter Wasserscheid. Liquid Organic Hydrogen Carriers as an efficient vector for the transport and storage of renewable energy. *International Journal of Hydrogen Energy*, 37(23):18118–18132, December 2012. doi: 10.1016/j.ijhydene.2012.08.066.
- [12] Alan Cooper. Reversible liquid carriers for an integrated production, storage and delivery of hydrogen. Technical report, U.S. Department of Energy, 2010. URL [https://www.hydrogen.energy.gov/pdfs/progress10/iii\\_14\\_cooper.pdf](https://www.hydrogen.energy.gov/pdfs/progress10/iii_14_cooper.pdf). U.S. DoE 2010 Annual Progress Report, III. Hydrogen Delivery.
- [13] Patrick Preuster, Christian Papp, and Peter Wasserscheid. Liquid Organic Hydrogen Carriers (LOHCs): Toward a Hydrogen-free Hydrogen Economy. *Accounts of Chemical Research*, 50(1):74–85, 2017. doi: 10.1021/acs.accounts.6b00474.
- [14] Axel Haupt and Karsten Müller. Integration of a LOHC storage into a heat-controlled CHP system. *Energy*, 118:1123–1130, 2017. ISSN 03605442. doi: 10.1016/j.energy.2016.10.129.
- [15] Farnaz Sotoodeh, Benjamin J.M. Huber, and Kevin J. Smith. Dehydrogenation kinetics and catalysis of organic heteroaromatics for hydrogen storage. *International Journal of Hydrogen Energy*, 37(3):2715–2722, February 2012. doi: 10.1016/j.ijhydene.2011.03.055.
- [16] H. Jorschick, M. Vogl, P. Preuster, A. Bösmann, and P. Wasserscheid. Hydrogenation of liquid organic hydrogen carrier systems using multicomponent gas mixtures. *International Journal of Hydrogen Energy*, 44(59):31172–31182, 2019. doi: 10.1016/j.ijhydene.2019.10.018.
- [17] Boris Brigljević, Manhee Byun, and Hankwon Lim. Design, economic evaluation, and market uncertainty analysis of LOHC-based, CO<sub>2</sub> free, hydrogen delivery systems. *Applied Energy*, 274:115314, 2020. doi: 10.1016/j.apenergy.2020.115314.
- [18] Ameya U. Pradhan, Anshu Shukla, Jayshri V. Pande, Shilpi Karmarkar, and Rajesh B. Biniwale. A feasibility analysis of hydrogen delivery system using liquid organic hydrides. *International Journal of Hydrogen Energy*, 36(1):680–688, 2011. doi: 10.1016/j.ijhydene.2010.09.054.
- [19] Craig Jensen, Daniel Brayton, Scott W. Jorgensen, and Peter Hou. Development of a Practical Hydrogen Storage System Based on Liquid Organic Hydrogen Carriers and a Homogeneous Catalyst. Technical report, U.S. Department of Energy, March 2017. doi: 10.2172/1347919. Last retrieved on 18/01/2022.
- [20] Matthias Niermann, Alexander Beckendorff, Martin Kaltschmitt, and Klaus Bonhoff. Liquid Organic Hydrogen Carrier (LOHC) – Assessment based on chemical and economic properties. *International Journal of Hydrogen Energy*, 44(13):6631–6654, 2019. doi: 10.1016/j.ijhydene.2019.01.199.
- [21] Teng He, Qijun Pei, and Ping Chen. Liquid organic hydrogen carriers. *Journal of Energy Chemistry*, 24(5):587–594, 2015. doi: 10.1016/j.jechem.2015.08.007.
- [22] Farnaz Sotoodeh, Benjamin J.M. Huber, and Kevin J. Smith. The effect of the N atom on the dehydrogenation of heterocycles used for hydrogen storage. *Applied Catalysis A: General*, 419-420:67–72, 2012.
- [23] Roland Peters, Robert Deja, Qingping Fang, Van Nhu Nguyen, Patrick Preuster, Ludger Blum, Peter Wasserscheid, and Detlef Stolten. A solid oxide fuel cell operating on liquid organic hydrogen carrier-based hydrogen – A kinetic model of the hydrogen release unit and system performance. *International Journal of Hydrogen Energy*, 44(26):13794–13806, 2019. doi: 10.1016/j.ijhydene.2019.03.220.
- [24] Jason Dennis, Thomas Bexten, Nils Petersen, Manfred Wirsum, and Patrick Preuster. Model-Based Analysis of a Liquid Organic Hydrogen Carrier (LOHC) System for the Operation of a Hydrogen-Fired Gas Turbine. *Journal of Engineering for Gas Turbines and Power*, 143(3):031011, 2021. doi: 10.1115/1.4048596.
- [25] Yikun Yang, Jing Yao, Huan Wang, Fusheng Yang, Zhen Wu, and Zaoxiao Zhang. Study on high hydrogen yield for large-scale hydrogen fuel storage and transportation based on liquid organic hydrogen carrier reactor. *Fuel*, 321:124095, 2022. doi: 10.1016/j.fuel.2022.124095.
- [26] Mengyan Zhu, Lixin Xu, Lin Du, Yue An, and Chao Wan. Palladium supported on carbon nanotubes as a high-performance catalyst for the dehydrogenation of dodecahydro-n-ethylcarbazole. *Catalysts*, 8, dec 2018. doi: 10.3390/catal8120638.
- [27] Yuan Dong, Ming Yang, Pan Mei, Chenguang Li, and Linlin Li. Dehydrogenation kinetics study of perhydro-n-ethylcarbazole over a supported pd catalyst for hydrogen storage application. *International Journal of Hydrogen Energy*, 41, jun 2016. doi: 10.1016/j.ijhydene.2016.03.157.
- [28] Zhaolu Feng and Xuefeng Bai. 3d-mesoporous kit-6 supported highly dispersed pd nanocatalyst for dodecahydro-n-ethylcarbazole dehydrogenation. *Microporous and Mesoporous Materials*, 335:111789, 2022. doi: 10.1016/j.micromeso.2022.111789.
- [29] Chao Wan, Yue An, Guohua Xu, and Wenjing Kong. Study of catalytic hydrogenation of N-ethylcarbazole over ruthenium catalyst. *International Journal of Hydrogen Energy*, 37(17):13092–13096, 2012. doi: 10.1016/j.ijhydene.2012.04.123.
- [30] Xufeng Ye, Yue An, and Guohua Xu. Kinetics of 9-ethylcarbazole hydrogenation over Raney-Ni catalyst for hydrogen storage. *Journal of Alloys and Compounds*, 509(1):152–156, 2011. doi: 10.1016/j.jallcom.2010.09.012.
- [31] S. Zrnčević and D. Rušić. Verification of the kinetic model for benzene hydrogenation by poisoning experiment. *Chemical Engineering Science*, 43(4):763–767, 1998. doi: 10.1016/0009-2509(88)80070-8.



- [32] Lars Peter Lindfors, Tapio Salmi, and Stefan Smeds. Kinetics of toluene hydrogenation on Ni/Al<sub>2</sub>O<sub>3</sub> catalyst. *Chemical Engineering Science*, 48(22):3813–3828, 1993. doi: 10.1016/0009-2509(93)80224-E.
- [33] R Vanmeerten. Gas phase benzene hydrogenation on a nickel-silica catalyst I. Experimental data and phenomenological description. *Journal of Catalysis*, 37(1):37–43, 1975. doi: 10.1016/0021-9517(75)90131-1.
- [34] Ming Yang, Yuan Dong, Shunxin Fei, Hanzhong Ke, and Hansong Cheng. A comparative study of catalytic dehydrogenation of perhydro-n-ethylcarbazole over noble metal catalysts. *International Journal of Hydrogen Energy*, 39(33):18976–18983, 2014. doi: 10.1016/j.ijhydene.2014.09.123.
- [35] Martin Eypasch, Michael Schimpe, Aastha Kanwar, Tobias Hartmann, Simon Herzog, Torsten Frank, and Thomas Hamacher. Model-based techno-economic evaluation of an electricity storage system based on Liquid Organic Hydrogen Carriers. *Applied Energy*, 185:320–330, 2017. doi: 10.1016/j.apenergy.2016.10.068.
- [36] Stephan Kiermaier, Daniel Lehmann, Andreas Bösmann, and Peter Wasserscheid. Dehydrogenation of perhydro-N-ethylcarbazole under reduced total pressure. *International Journal of Hydrogen Energy*, 46(29):15660–15670, 2021. doi: 10.1016/j.ijhydene.2021.02.128.
- [37] H. Jorschick, P. Preuster, S. Dürr, A. Seidel, K. Müller, A. Bösmann, and P. Wasserscheid. Hydrogen storage using a hot pressure swing reactor. *Energy & Environmental Science*, 10(7):1652–1659, 2017. doi: 10.1039/C7EE00476A.
- [38] H. Jorschick, S. Dürr, P. Preuster, A. Bösmann, and P. Wasserscheid. Operational Stability of a LOHC-Based Hot Pressure Swing Reactor for Hydrogen Storage. *Energy Technology*, 7(1):146–152, 2019. doi: 10.1002/ente.201800499.
- [39] W. Peters, M. Eypasch, T. Frank, J. Schwerdtfeger, C. Körner, A. Bösmann, and P. Wasserscheid. Efficient hydrogen release from perhydro-N-ethylcarbazole using catalyst-coated metallic structures produced by selective electron beam melting. *Energy & Environmental Science*, 8(2):641–649, 2015. doi: 10.1039/C4EE03461A.
- [40] J. T. Miller, B. L. Meyers, F. S. Modica, G. S. Lane, M. Vaarkamp, and Koningsberger D. C. Hydrogen temperature-programmed desorption (H<sub>2</sub> TPD) of supported platinum catalysts. *Journal of Catalysis*, 143:14, 1993. doi: 10.1006/jcat.1993.1285.
- [41] J. E. House. *Principles of chemical kinetics*. Elsevier/Academic Press, Amsterdam; Boston, 2 edition, 2007. ISBN 978-0-12-356787-1.
- [42] M Gambini. Metal hydride energy systems performance evaluation. Part A: Dynamic analysis model of heat and mass transfer. *International Journal of Hydrogen Energy*, 19(1):67–80, 1994. doi: 10.1016/0360-3199(94)90179-1.
- [43] P Muthukumar, U Madhavakrishna, and A Dewan. Parametric studies on a metal hydride based hydrogen storage device. *International Journal of Hydrogen Energy*, 32(18):4988–4997, 2007. doi: 10.1016/j.ijhydene.2007.08.010.
- [44] In Young Choi, Byeong Soo Shin, Sang Kyu Kwak, Kyung Soo Kang, Chang Won Yoon, and Jeong Won Kang. Thermodynamic efficiencies of hydrogen storage processes using carbazole-based compounds. *International Journal of Hydrogen Energy*, 41(22):9367–9373, 2016. doi: 10.1016/j.ijhydene.2016.04.118.
- [45] Norbert Heublein, Malte Stelzner, and Thomas Sattelmayer. Hydrogen storage using liquid organic carriers: Equilibrium simulation and dehydrogenation reactor design. *International Journal of Hydrogen Energy*, 45:15, 2020. doi: 10.1016/j.ijhydene.2020.04.274.
- [46] Byeong Soo Shin, Chang Won Yoon, Sang Kyu Kwak, and Jeong Won Kang. Thermodynamic assessment of carbazole-based organic polycyclic compounds for hydrogen storage applications via a computational approach. *International Journal of Hydrogen Energy*, 43(27):12158–12167, 2018. doi: 10.1016/j.ijhydene.2018.04.182.
- [47] H.Scott Fogler. *Elements of chemical reaction engineering*. Prentice Hall International Series in the Physical and Chemical Engineering Sciences, 2016.
- [48] S. Dürr, S. Zilm, M. Geißelbrecht, Karsten Müller, P. Preuster, A. Bösmann, and P. Wasserscheid. Experimental determination of the hydrogenation/dehydrogenation - equilibrium of the lohc system H<sub>0</sub>/H<sub>18</sub>-dibenzyltoluene. *International Journal of Hydrogen Energy*, 46:12, 2021. doi: 10.1016/j.ijhydene.2021.07.119.